NOAA Technical Report NESDIS 122

JCSDA Community Radiative Transfer Model (CRTM) - Version 1

Washington, D.C.
August 2006

U.S. DEPARTMENT OF COMMERCE
National Oceanic and Atmospheric Administration
National Environmental Satellite, Data, and Information Service

NOAA TECHNICAL REPORTS

National Environmental Satellite, Data, and Information Service

The National Environmental Satellite, Data, and Information Service (NESDIS) manages the Nation's civil Earth-observing satellite systems, as well as global national data bases for meteorology, oceanography, geophysics, and solar-terrestrial sciences. From these sources, it develops and disseminates environmental data and information products critical to the protection of life and property, national defense, the national economy, energy development and distribution, global food supplies, and the development of natural resources.

Publication in the NOAA Technical Report series does not preclude later publication in scientific journals in expanded or modified form. The NESDIS series of NOAA Technical Reports is a continuation of the former NESS and EDIS series of NOAA Technical Reports and the NESC and EDS series of Environmental Science Services Administration (ESSA) Technical Reports.

A limited number of copies are available by contacting Jessica Pejsa, NOAA/NESDIS, E/RA3, 5200 Auth Road, Room 601, Camp Springs, Maryland 20746, (301) 763-8184 x115. Copies can also be ordered from the National Technical Information Service (NTIS), U.S. Department of Commerce, Sills Bldg., 5285 Port Royal Road, Springfield, VA 22161, (703) 487-4650 (prices on request for paper copies or microfiche, please refer to PB number when ordering). A partial listing of more recent reports appear below:

NESDIS 88 Analytical Model of Refraction in a Moist Polytropic Atmosphere for Space and Ground-Based GPS Applications. Simon Rosenfeld, April 1997.

NESDIS 89 A GOES Image Quality Analysis System for the NOAA/NESDIS Satellite Operations Control Center. Donald H. Hillger and Peter J. Celone, December 1997.

NESDIS 90 Automated Satellite-Based Estimates of Precipitation: An Assessment of Accuracy. Michael A. Fortune, June 1998.

NESDIS 91 Aliasing of Satellite Altimeter Data in Exact-Repeat Sampling Mode: Analytic Formulas for the Mid-Point Grid. Chang-Kou Tai, March 1999.

NESDIS 92 Calibration of the Advanced Microwave Sounding Unit-A Radiometers for NOAA-L and NOAA-M. Tsan Mo, May 1999.

NESDIS 93 GOES Imager and Sounder Calibration, Scaling, and Image Quality. Donald W. Hillger, June 1999.

NESDIS 94 MSU Antenna Pattern Data. Tsan Mo, Thomas J. Kleespies, and J. Philip Green, March 2000.

NESDIS 95 Preliminary Findings from the Geostationary Interferometer Observing System Simulation Experiments (OSSE). Bob Aune, Paul Menzel, Jonathan Thom, Gail Bayler, Allen Huang, and Paolo Antonelli, June 2000.

NESDIS 96 Hydrography of the Ross Sea Continental Shelf During the Roaverrs, NBP96-06, Cruise December 1996 - January 1997. Michael L. Van Woert, David Pryor, Eric Quiroz, Richard Slonaker, and William Stone, September 2000.

NESDIS 97 Hydrography of the Ross Sea Continental Shelf During the Roaverrs, NBP97-09, Cruise December 1997 - January 1998. Michael L. Van Woert, Lou Gordon, Jackie Grebmeier, Randal Holmbeck, Thomas Henderson, and William F. Van Woert, September 2000.

NOAA Technical Report NESDIS 122

JCSDA Community Radiative Transfer Model (CRTM) - Version 1

Yong Han[1,2], Paul van Delst[1,4] , Quanhua Liu[1,5], Fuzhong Weng[1,2], Banghua Yan[1,5], Russ Treadon[1,3] and John Derber[1,3]

1. Joint Center for Satellite Data Assimilation, Camp Springs, MD
2. NOAA/NESDIS/Center for Satellite Applications and Research, Camp Springs, MD
3. NOAA/NWS/NCEP/Environmental Modeling Center
4. CIMSS/SSEC, University of Wisconsin-Madison
5. QSS Group, Inc.

Washington, DC
December 2005

U.S. DEPARTMENT OF COMMERCE
Carlos M. Gutierrez, Secretary

National Oceanic and Atmospheric Administration
Vice Admiral Conrad C. Lautenbacher, Jr., U.S. Navy (Ret.), Under Secretary

National Environmental Satellite, Data, and Information Service
Gregory W. Withee, Assistant Administrator

TABLE OF CONTENTS

LIST of TABLES

LIST OF FIGURES

Preface

The development of fast and accurate radiative transfer models for clear atmospheric conditions has enabled the direct assimilation of clear sky radiances from satellites in numerical weather prediction models. Currently, many fast models also handle the scattering and emission processes that dominate cloud and precipitation. Some analytic Jacobian schemes, crucial components for satellite data assimilation, have also been developed. For the operational data assimilation system, distinct features from each radiative transfer model may ultimately be combined in the more refined versions of the scattering radiative transfer by taking the advantages of speed and accuracy relative to benchmark solutions, storage efficiency for coefficients, inclusion of Jacobian, and potential developments for future instruments.

This report documents the theoretical background and functional implementation of the first version of the Community Radiative Transfer Model (CRTM), developed at the U.S. Joint Center for Satellite Data Assimilation (JCSDA) with algorithm and software input from JCSDA-funded research institutions. As a technical lead and point of contact in JCSDA radiative transfer science priority area, I would like to praise our radiative transfer team for their diligent work and dedication to the timeliness release of the CRTM to the JCSDA partners.

This version-1 CRTM simulates the microwave and infrared radiances observed by instruments on board spacecraft for a given state of the atmosphere and Earth's surface. It includes components that compute the gaseous absorption of radiation, absorption and scattering of radiation by hydrometeors and aerosols, and emission and reflection of radiation by ocean, land, snow and ice surfaces. All of these component results are then used to perform accurate radiative transfer to yield simulated satellite sensor radiances. In addition to the forward model, the corresponding tangent linear, adjoint and K-Matrix models have also been developed and included in the CRTM package for calculations of the radiance sensitivities with respect to the state variables. The software was designed with a balance between the computational efficiency and flexibility for future extension and improvement.

Dr. Fuzhong Weng, Chief
Sensor Physics Branch
Satellite Meteorology and Climatology Division
Center for Satellite Applications and Research
NOAA/NESDIS
5200 Auth Road, Room 712
Camp Springs, MD 20746
USA

1 Introduction

This document describes the theoretical background and functional implementation of the first version Community Radiative Transfer Model (CRTM), developed at the Joint Center for Satellite Data Assimilation (JCSDA). The CRTM User Guide is available from http://www.jcsda.noaa.gov/crtm. The CRTM simulates the microwave (MW) and infrared (IR) radiances observed by instruments on board spacecraft for a given state of the atmosphere and Earth's surface. It also computes radiance sensitivities such as the radiance derivatives (Jacobians) with respect to the state variables. It is an essential component of the Gridpoint Statistical Interpolation (GSI) data assimilation system at the NOAA National Center for Environmental Prediction (NCEP) Environmental Modeling Center (EMC). The CRTM can also be used for other satellite radiance applications where fast and accurate simulated satellite sensor radiances are required; such as radiance data inversions for state variables. Many MW and IR sensors are supported within the CRTM.

The development of the CRTM was stimulated by recent research activities in the radiative transfer (RT) modeling community. Improvement in modeling satellite radiances is one of the JCSDA research priorities so as to fully utilize the information of satellite measurements under all weather conditions for numerical weather prediction (NWP). For example, cloud affected satellite radiances have not been assimilated into operational forecast models although the measurements contain considerable information pertinent to the atmospheric hydrological cycle. The use of cloudy radiances in NWP models will ultimately enhance the impacts that have been demonstrated presently through clear radiance assimilation and add to our knowledge of clouds, the surface and the hydrological cycle. The CRTM implements many recent achievements to improve the modeling of cloudy and aerosol-affected satellite radiances. Another important purpose of developing the new model was to design a framework for research groups and developers to simplify the implementation of experimental algorithms and allow it to be easily tested and evaluated in the operational environment and thereby accelerate the transition from research to operational application.

The earlier RT models used at the JCSDA were all emission-based, applicable only to clear sky conditions (Kleespies et al., 2004). There was also no built-in component to compute the surface emissivity and reflectivity. In addition, the software was not flexible enough to meet our development requirements for adding additional functionality. The CRTM has improved upon the earlier models in both the scientific and software aspects. It takes into account the absorption and scattering from various types of hydrometoers and aerosols, as well as including a comprehensive set of models for computing surface emissivity and reflectivity over land, ocean, ice and snow surfaces for both the microwave and infrared spectral regions[1]. The CRTM software framework was designed to strike a balance between computational efficiency[2], code maintenance, and flexibility for future improvements and extensions. The source code is written in standard Fortran95 and makes extensive use of modules and derived type data structures to achieve these goals.

[1] Modeling of other spectral regions (e.g. visible, UV) can also be easily included.
[2] Including memory management.

2 CRTM Components

Simulation of atmospheric radiative transfer involves a number of physical processes. One of the main goals of the CRTM framework is to provide for the development of models for these processes independently of any other. The components of the radiative transfer processes considered by the CRTM are loosely divided into four main categories,

1. Absorption of radiation by the gaseous constituents of the atmosphere,
2. Absorption and scattering of radiation by clouds[3] and aerosols,
3. Surface emission of radiation and surface interaction with downwelling atmospheric radiation, and
4. Solution of the radiative transfer equation.

In some cases the above are further split into subcategories, e.g. cloud and aerosol scattering are treated separately, surface optics is split into both surface types and spectral subcategories, etc. The CRTM framework was designed to allow for a relatively natural division of the software implementation of the above categories into modular entities (see Figure 1) so that as new or updated algorithms are developed, they can be easily integrated.

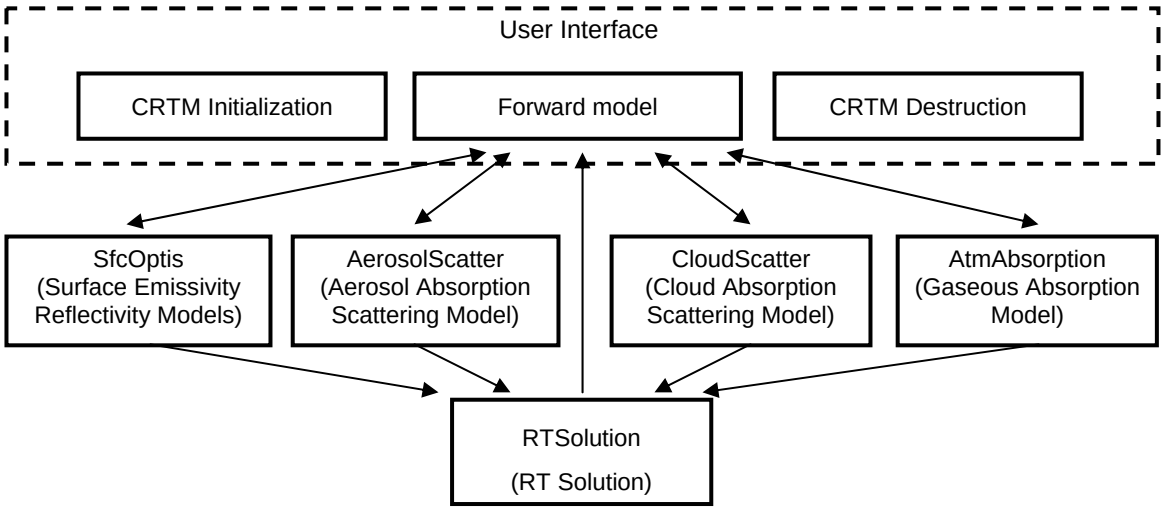

Figure 1 CRTM forward model module diagram

2.1 Gaseous absorption model

The gaseous absorption model is the main component of the CRTM and drives the computation. Currently the CRTM is setup for a polychromatic gas absorption model, but work is also proceeding on a monochromatic model.

[3] The term hydrometeor is probably more appropriate as precipitation is also considered in the CRTM.

The polychromatic gas absorption model begins with the channel layer-to-space transmittance, T_{ch}, which is defined as the convolution of the monochromatic transmittance, $T(\nu)$, with the channel spectral response function (SRF), $\phi(\nu)$:

$$T_{ch} = \int_{\Delta\nu} T(\nu)\phi(\nu)d\nu \qquad (1)$$

Currently it is implemented with a special version of the Optical Path TRANsmittance (OPTRAN) (McMillin et al., 1995). A distinct characteristic of the OPTRAN model is that the transmittances of an absorbing gas are estimated at levels of the absorber's integrated amount, rather than at the fixed pressure levels (Saunders, et al., 1999). In other words, the OPTRAN transmittances are estimated in absorber space, not in pressure space. One of the advantages using the absorber space is that transmittances can be predicted accurately with fewer predictors than using the pressure space.

Over the past twenty years, OPTRAN has experienced considerable development. In 1998, OPTRAN with version 6 (OPTRAN-v6) was for the first time applied in the NCEP satellite data assimilation system (Kleespies et al., 2004). Afterwards, two new versions have been developed simultaneously. One version, referred as OPTRAN-v7, adopts a new technique to take the polychromatic effects into account when computing the radiances with finite bandwidth (Xiong et al., 2005). The other version, referred as Compact OPTRAN (so named due to its high efficiency in using computer memory resource) improves vertical structures of the Jacobian profiles by constraining the variations of the transmittance regression coefficients between different vertical levels. The Compact OPTRAN is the one currently implemented in the CRTM. It was primarily developed by Dr. Yoshikiko Tahara, a visiting scientist from JMA, Japan in 2002 and 2003. Since the algorithm has not been published in open literature, a detailed description is given below.

Let $T_w(\nu)$ and $T_o(\nu)$ be the monochromatic transmittances of water vapor and ozone, respectively, and $T_d(\nu)$ the transmittance of the dry gas, which is a collective component including all the absorbing gases except water vapor and ozone. Then the total monochromatic transmittance can be expressed as the product of these three components:

$$T(\nu) = T_w(\nu)T_o(\nu)T_d(\nu). \qquad (2)$$

We may also express the total channel transmittance T_{ch} defined in (1) in a similar form through introducing the concept of the effective transmittances:

$$T_{ch} = T_{ch,w}T^*_{ch,o}T^*_{ch,d}, \qquad (3)$$

where $T_{ch,w}$ is the channel transmittance of water vapor, defined as

$$T_{ch,w} = \int T_w(\nu)\phi(\nu)d\nu, \qquad (4)$$

and $T^*_{ch,d}$ and $T^*_{ch,o}$ are the effective channel transmittances of the dry gas and ozone, respectively. The effective dry gas $T^*_{ch,d}$ is defined as

$$T^*_{ch,d} = T_{ch,d+w} / T_{ch,w}, \qquad (5)$$

where $T_{ch,d+w}$ is the channel transmittance of the combined dry gas and water vapor:

$$T_{ch,d+w} = \int T_d(\nu) T_w(\nu) \phi(\nu) d\nu , \quad (6)$$

and the effective ozone transmittance $T^*_{ch,o}$ is defined as

$$T^*_{ch,o} = T_{ch} / T_{ch,d+w} . \quad (7)$$

Equation (3) is used to derive the channel transmittance. The three transmittance components $T_{ch,w}$, $T^*_{ch,d}$ and $T^*_{ch,o}$ are estimated using the regression technique described in the following.

For simplicity, let the index *i* represent water vapor, ozone or dry gas and $T_{ch,i}(A_i)$ one of the three transmittance components, $T_{ch,w}$, $T^*_{ch,d}$ and $T^*_{ch,o}$, at the level with the integrated absorber amount A_i (from space to the pressure level *p*), which is computed as

$$A_i = \int_0^p \frac{r_i}{g \cos(\theta)} dp' , \quad (8)$$

where r_i is the gas specific amount, θ the zenith angle and *g* the gravitation constant. With the symbols defined, the transmittance is calculated as

$$T_{ch,i}(A_i) = e^{-\int_0^{A_i} k_{ch,i}(A_i') dA_i'} , \quad (9)$$

where

$$Ln(k_{ch,i}(A_i)) = c_{i,0}(A_i) + \sum_{j=1}^{6} c_{i,j}(A_i) x_{i,j}(A_i) ,$$

In (9), $k_{ch,i}(A_i)$ is the absorption coefficient and *Ln()* is the natural logarithm. The predictors $x_{i,j}(A_i)$ ($j = 1, 6$) are functions of atmospheric state variables and the coefficients $c_{i,0}(A_i)$ and $c_{i,j}(A_i)$ are polynomial functions of A_i in the form:

$$c_{i,j}(A_i) = \sum_{n=0}^{N} a_{i,j,n} Ln(A_i)^n , \quad (10)$$

where $a_{i,j,n}$ are the regression coefficients (also referred as transmittance coefficients). The set of 6 predictors varies among different channels and is selected from a 29-predictor pool, as listed in Table 1. The predictor pool includes 11 standard predictors, which are not specific to any of the three transmittance components, and 18 integrated predictors, which are evenly divided into three subsets, each belonging to a particular transmittance component. Let *u* represent the atmosphere pressure *P* or temperature *T*; the integrated predictors for the component *i* may be expressed as

$$u_i^*(A_i) = \frac{\int_0^{A_i} u(A_i') dA_i'}{\int_0^{A_i} dA_i'} ,$$

$$u_i^{**}(A_i) = \frac{\int_0^{A_i} u(A_i')A_i' dA_i'}{\int_0^{A_i} A_i' dA_i'} \text{ , and}$$

$$u_i^{***}(A_i) = \frac{\int_0^{A_i} u(A_i')A_i'^2 dA_i'}{\int_0^{A_i} A_i'^2 dA_i'} \text{ .} \qquad (11)$$

The transmittance coefficients, $a_{i,j,n}$ in (10) are obtained through a training process with a statistical data ensemble, in which predictands and predictors are calculated from a set of diversified atmospheric profiles. For the dry gas component, the mixing ratio profile does not change among different atmospheric states. Because of this the dry gas is also called fixed gas. An exhausting search is performed for each gas component and channel to select the best set of predictors and order N (<=10) of the polynomial function, which minimize the fitting residual. Low order is taken if the fitting accuracy is not degraded significantly for better computational stability. In addition, an automated procedure is adopted to make sure that the set of predictors with strong correlations between the selected predictors is not selected, which may cause the transmittance calculation unstable.

The use of the polynomial functions in (10) for the regression coefficients in (9) is a unique feature of the Compact OPTRAN. It may be considered as applying the polynomial functions to constrain the shapes of the coefficient vertical profiles. As a result, unrealistic sawtooth-like structures of the Jacobian profiles which may occur with the unconstrained fast transmittance algorithms are avoided, especially for the channels with a weak gaseous absorption. Another good feature of the algorithm, especially for hyperspectral sensors, is the small size of the regression coefficients required to compute a transmittance profile for a given channel and gas component. Compared with other fast transmittance algorithms (e.g. OPTRAN-v6 and OPTRAN-v7), which require a different set of coefficients at each of the profile levels, the Compact OPTRAN uses only a small fraction of the number of coefficients used in these algorithms, saving significant amount of computer space.

The fitting errors for HIRS and AMSU channels on NOAA 16 are shown in Fig. 2 and Fig. 3. The fitting errors are measured with the brightness temperature calculated with the radiative transfer under a clear-sky condition. On average, the errors are less than 0.1 K. In Fig. 4, several Jacobian profiles for HIRS channels are shown, which are compared with those obtained from LBLRTM (Clough et al., 1992) by using the perturbations (finite-difference) method.

Standard Predictors		Integrated predictors			
1	T	1	T_w*	12	P_o***
2	P	2	T_w**	13	T_d*
3	T^2	3	T_w***	14	T_d**
4	P^2	4	P_w*	15	T_d***
5	$T\,P$	5	P_w**	16	P_d*
6	$T^2\,P$	6	P_w***	17	P_d**
7	$T\,P^2$	7	T_o*	18	P_d***
8	$T^2\,P^2$	8	T_o**		
9	$\sqrt[4]{P}$	9	T_o***		
10	Q	10	P_o*		
11	$Q/\sqrt{T}$	11	P_o**		

Table 1 Standard and integrated predictors

- see equation 11 for their definition
- T – temperature; P – pressure; Q – water vapor mixing ratio

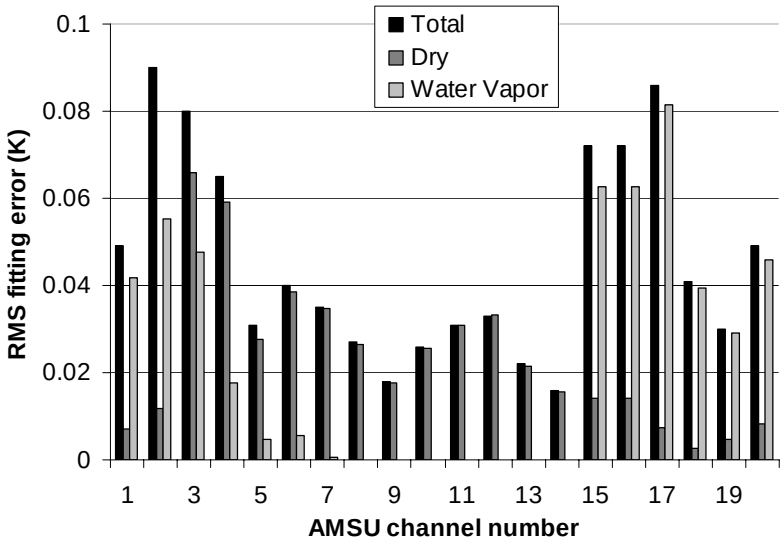

Figure 2 RMS fitting errors for AMSU on NOAA-16

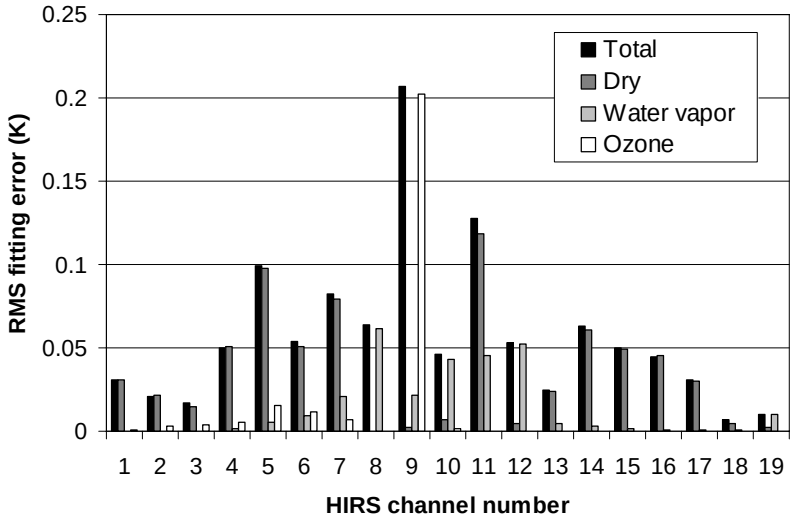

Figure 3 RMS fitting errors for HIRS/3 on NOAA-16

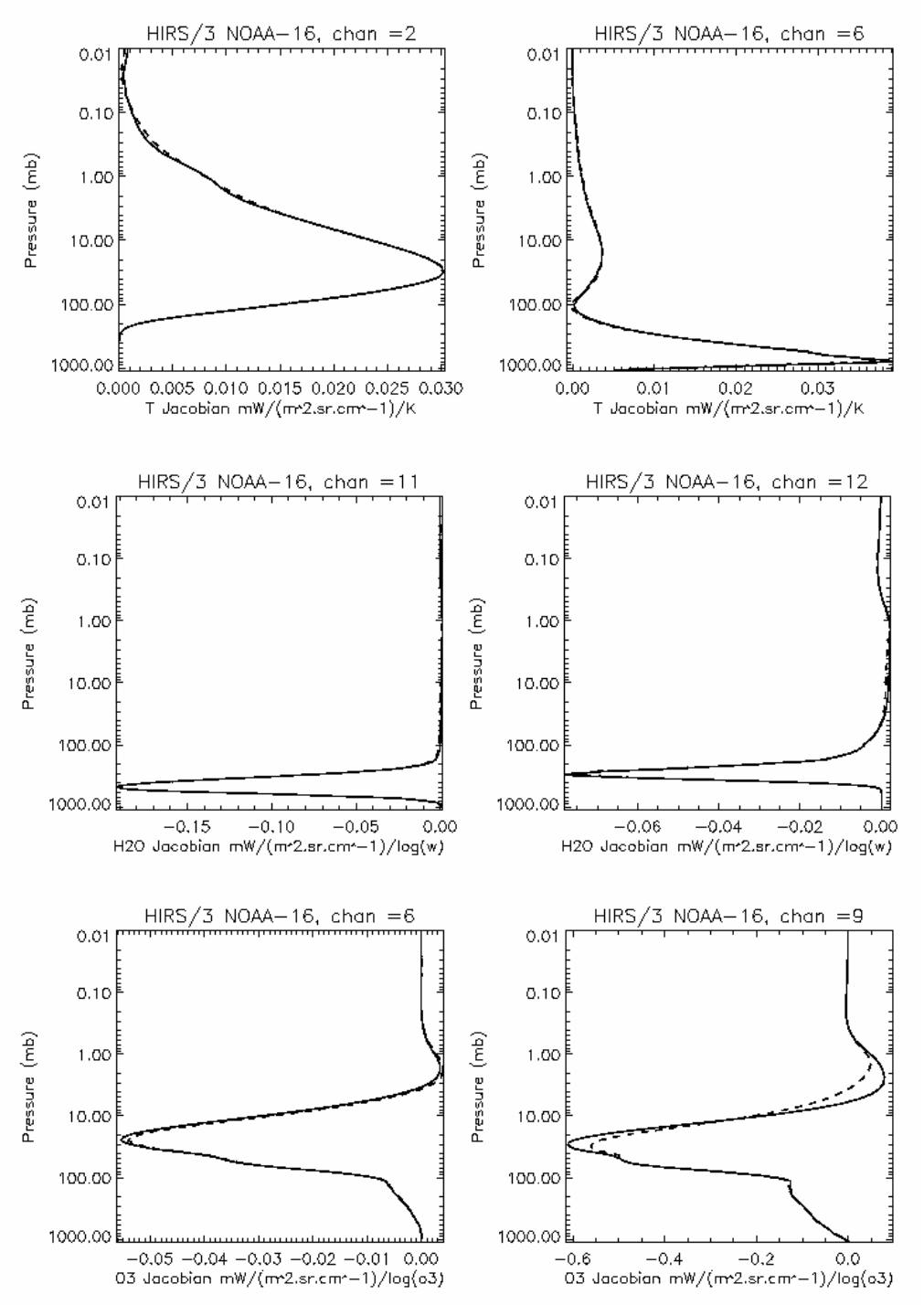

Figure 4 Jacobians with respect to temperature (upper panel), water vapor (middle panel) and ozone (bottom panel) at selected HIRS channels under clear sky condition.

- Solid line – OPTRAN; dashed – line-by-line model.

2.2 Surface Emissivity and Reflectivity Models

The CRTM employs a suit of IR and MW surface emissivity and reflectivity models covering land, ocean, ice and snow surfaces. Some of the models are physically based while others are empirical or semi-empirical. The CRTM also has an option allowing the users to input their own emissivity and direct reflectivity spectrum.

2.2.1 IR Sea Surface Emissivity Model

The IR sea surface emissivity model utilizes a lookup table (LUT) of sea surface emissivities derived from the emissivity model for a wind-roughened sea surface (Wu and Smith, 1997). The sea surface is modeled by numerous small facets whose slopes approximately follow the normal and isotropic distribution (Cox and Munk, 1954). Each of the facets is treated as a specular surface and emission at the observation angle is computed with the geometrical optics, with wave shadowing effects and surface reflection of surface emission taken into account. The lookup table variables are zenith angle(67 from nadir to 66.5°), frequency (153 from 600-3000cm^{-1}), and wind speed (23 from 0-15ms^{-1}). Currently linear interpolation is performed between LUT values.

2.2.2 IR Surface Emissivity Database

The IR surface emissivity used over land, snow and ice is provided by an emissivity database (Carter et al., 2002). The database contains surface reflectance measurements as a function of wavelength in both visible and IR spectral regions for the 24 surface types listed in Table 2. The emissivity is calculated as one minus the reflectance under the assumption of a Lambertian surface in the IR spectral region.

Surface Type	
Compacted soil	Grass scrub
Tilled soil	Oil grass
Sand	Urban concrete
Rock	Pine brush
Irrigated low vegetation	Broadleaf brush
Meadow grass	Wet soil
Scrub	Scrub soil
Broadleaf forest	Broadleaf(70)/Pine(30)
Pine forest	Water
Tundra	Old snow
Grass soil	Fresh snow
Broadleaf/Pine forest	New ice

Table 2 Surface types included in the IR emissivity database

2.2.3 MW Ocean Emissivity Model

The MW emissivity over ocean surface is computed using FASTEM-1 (English and Hewison, 1998). The model treats the surface emissivity in three categories: specular reflection and the modulation from large and small scales depending on wind speed and frequency of electromagnetic wave. It takes satellite zenith angle, water temperature, surface wind speed, and frequency as model inputs and computes surface emissivity at vertical (V) and horizontal (H) polarizations.

2.2.4 MW Land Emissivity Model

The MW land emissivity model (LandEM) computes land surface emissivity for various surface types, including snow, deserts and vegetation using the two-stream radiative approximation (Weng, et al, 2001). The reflection and emission occurring at the interfaces above and below the scattering layer are taken into account and the cross polarization and attenuation due to surface roughness are parameterized as a function of roughness height and frequency. For the vegetation canopy the optical parameters are derived using geometric optics. For a medium with a higher fractional volume of particles such as snow and deserts, the scattering and absorption coefficients are approximated using the dense medium theory. The model takes satellite zenith angle, MW frequency, soil moisture content, vegetation fraction, soil temperature, land surface temperature and snow depth as inputs and computes surface emissivity at V and horizontal H polarizations. As an example, Figs. 5(a) and (b) display the microwave surface emissivity spectra over several surface conditions in a local zenith angle of 53 degree for V- and H- polarizations, respectively. In the figure, the emissivity spectra over snow, canopy, bare soil, wet land, desert conditions are simulated using LandEM, whereas the ocean surface emissivity are simulated using the MW ocean emissivity model for comparison.

LandEM is applied according the following conditions:

<u>Over land</u>

If the frequency < 80 GHz, the emissivity is given by LandEM and otherwise emissivity(V and H polarizations) = 0.95.

<u>Over snow</u>

When the snow empirical model (see the next section) is not invoked, if the frequency < 80 GHz, the emissivity is given by LandEM and otherwise emissivity(V and H polarizations) = 0.90.

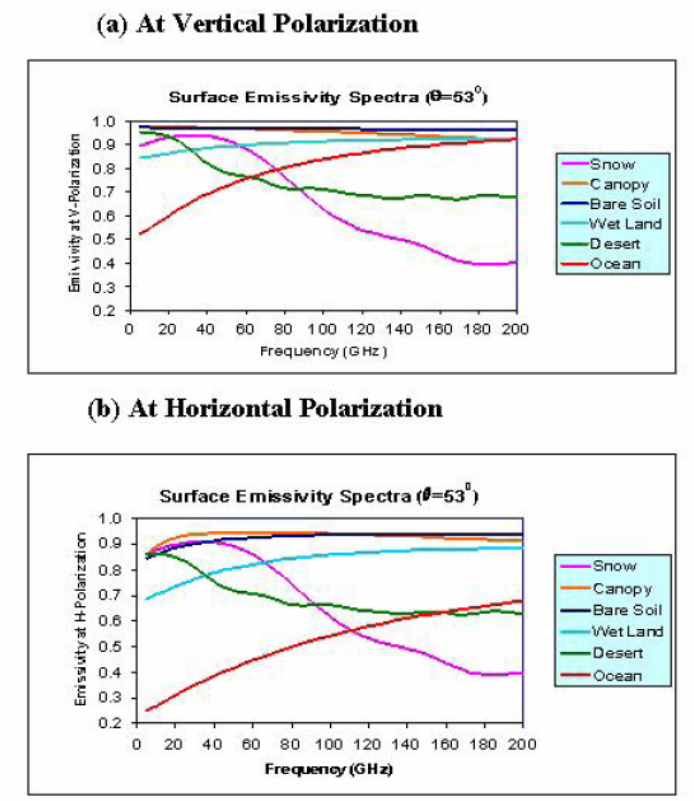

Figure 5 Microwave emissivity spectra as a function of frequency.

2.2.5 MW Empirical Emissivity Models over Snow and Ice Surfaces

The empirical snow and ice emissivity models take an empirical approach to compute the emissivity via a combination of satellite window channel observations and emissivity databases collected from ground-based microwave instruments (Yan and Weng, 2004). The emissivity databases contain sets of emissivity spectral data measured at a zenith view angle of 50 degree for various surface types. Currently two such databases have been established, one for snow surfaces and the other ice surfaces. For demonstration, Figs. 6(a) and (b) show the sets of the weighted emissivity spectra over various snow and sea ice surfaces, respectively. The window channel observations are used to identify the snow or ice surface type that best describes the surface condition observed by the window channels. Thus, a key component in the model is the relationship that maps the window channel observations to the snow or ice surface type (Yan and Weng, 2004). The mapping algorithms have been developed for several MW sensors listed in Table 3. Once a spectrum is identified, it is then adjusted for the requested zenith angle by using LandEM (Weng, et al, 2001).

For those sensors not listed in the table, or when the window channel measurements are not available, the snow surface emissivity is computed with LandEM and the ice surface emissivity (V and H polarizations) is set with a value of 0.92.

Sensor Name	Surface	Required channels
AMSUA	Ice, Snow	1, 2, 3, 4
AMSUB	Ice, Snow	1, 2
AMSRE	Ice, Snow	1 to 12
SSMI	Ice, Snow	1 to 7

Table 3 MW sensors supported by the empirical emissivity model

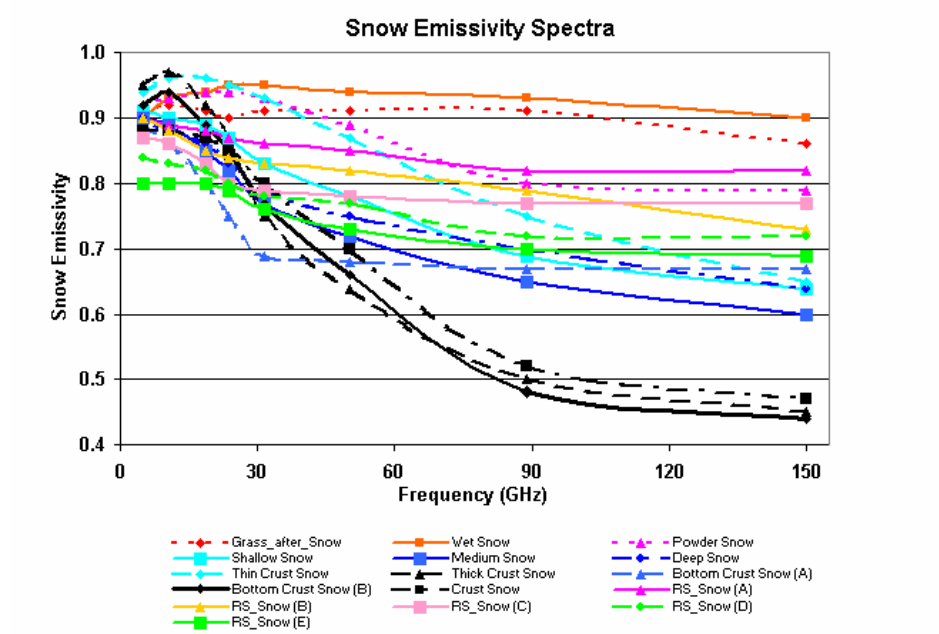

(A)

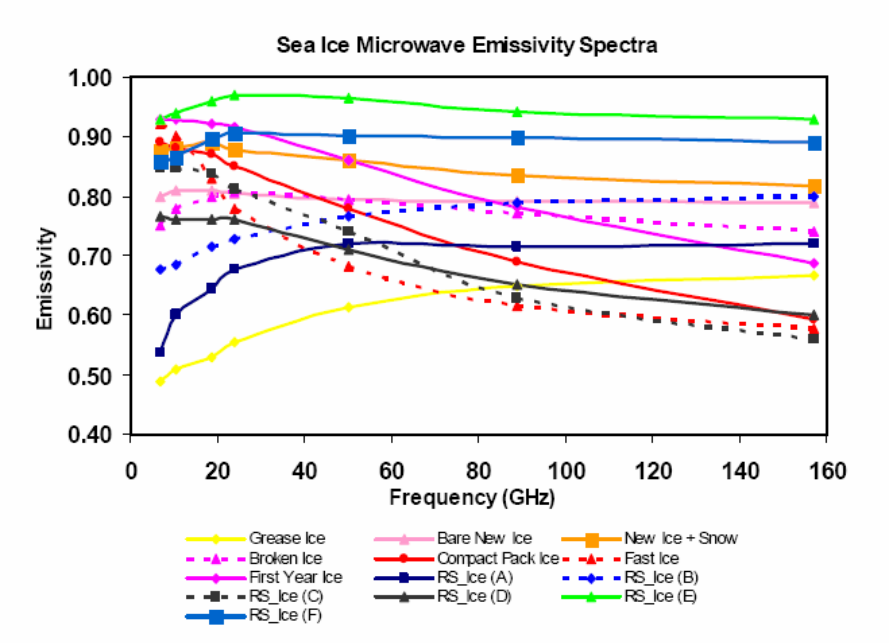

(B)

Figure 6 Microwave emissivity spectra as a function of frequency. (a) Various snow emissivity spectra across the range between 4.9 and 150 GHz. (b) Various sea ice emissivity spectra across the range between 6 and 157 GHz.

2.3 Cloud Optical Parameter Lookup Table

Cloud optical parameters are calculated with the general Mie theory using a modified gamma distribution function. The parameters such as extinction coefficients, single scattering albedo and phase matrix elements are pre-calculated and stored in a lookup table. This table is searched with particle mean size and cloud water content (or mixing ratio). Note that the phase matrix elements are decomposed into a series of Legendre polynomials and the coefficients associated with the polynomials are also stored in the table. Data for liquid water cloud, ice cloud, rain cloud, snow, graupel, and hail are all included. Cloud liquid and ice are treated differently through specifications of water or ice permittivity. The IR optical parameters for non-spherical cirrus clouds are adopted from the data set calculated by the finite-difference time domain method (Yang et al., 2001).

2.4 Radiative Transfer Solver

The RT solver module solves the RT equation for given atmospheric optical depth profile, surface emissivity and reflectivity, cloud optical parameters and source functions. The clear and cloudy cases are treated with different methods, allowing a simple and efficient solution under the clear-sky condition.

2.4.1 Basic Radiative Transfer Equation

Assuming a vertically-stratified, plane-parallel and non-polarized atmosphere, the monochromatic radiative transfer equation may be written as

$$\mu \frac{dI(\tau;u,\phi)}{d\tau} = I(\tau;u,\phi) - \frac{\varpi}{4\pi}\int P(\tau;u,\phi;u',\phi')I(\tau;u',\phi')du'd\phi' - \frac{\varpi}{4\pi}P(\tau;u,\phi;-u_{\otimes},\phi_{\otimes})F_{\otimes}e^{-\tau/\mu_{\otimes}} - (1-\varpi)B(T)) \quad (13)$$

where I is the intensity, τ the optical depth, B the Planck function, P the phase function, and ϖ the single-scattering albedo. The directions of the incoming and outgoing light beams are represented by (μ',ϕ') and (μ,ϕ), where $\mu' = \cos(\theta')$ and $\mu = \cos(\theta)$, θ' and θ are the zenith angles and ϕ' and ϕ the azimuthal angles. In the third term on the right side of (13), $F_{\otimes}$ is the solar irradiance incident at the direction $(-\mu_{\otimes},\phi_{\otimes})$, where the minus sign represents the downward propagation. For simplicity, the wavelength subscript is omitted in the equation.

2.4.2 Atmospheric Layering Scheme

In the discrete ordinate system, the atmosphere is divided into layers. The CRTM adopts an atmospheric layering scheme shown in Fig. 7, in which the state variables such as the temperature and water vapor are layer means, whose vertical coordinates are given by the layer pressures. The level pressures at the layer boundaries are also required input variables. The atmospheric profiles are

stored in arrays with the pressures in ascending order. The CRTM does not require a fixed number of layers and layer thicknesses, except that the top pressure level needs to be set at 0.005 hPa. It is the user's responsibility to supply a meaningful atmospheric profile.

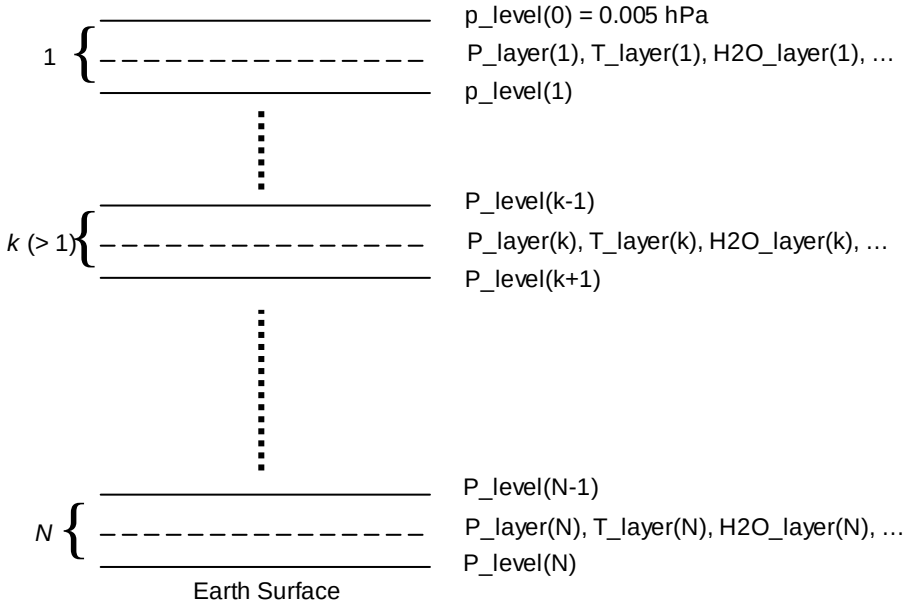

Figure 7 Atmosphere profile layering scheme.

- P_level(k) – level pressure, P_layer(k) – layer pressure (P_level(k-1) < P_layer(k) < P_level(k)), T_layer(k) – layer temperature and H_2O_layer(k) – layer water vapor. The number of layers and the layer thicknesses are determined by the user.

2.4.3 RT Solution under Clear-Sky Conditions

When the sky is clear, $\varpi \approx 0$, and the scattering terms in (13) are neglected in the MW and IR regions. The solution for the monochromatic intensity can then be written in the form:

$$I(\mu) = [r\int_0^{\tau_N} B(T)d\mathrm{T}_d(\tau',\mu_d) + r_\otimes \frac{F_\otimes}{\pi}\mathrm{T}_d(0,\mu_\otimes) + \varepsilon B(T_s)]\mathrm{T}_u(\tau_N,\mu) - \int_0^{\tau_N} B(T)d\mathrm{T}_u(\tau',\mu), \quad (14)$$

where τ_N is the optical depth from the top to bottom of the atmosphere, $\mathrm{T}_u(\tau,\mu) = e^{-\tau/\mu}$ and $\mathrm{T}_d(\tau,\mu) = e^{-(\tau_N-\tau)/|\mu|}$ are respectively the upwelling and dowelling transmittances, ε the surface emissivity, and r and $r_\otimes$ the surface reflectivity. The first term on the right side of (14) is the atmospheric downwelling radiation reflected by the Earth's surface. The second term is the surface-reflected solar radiation and is neglected in the MW region. The third term is the contribution of the surface emission at the skin temperature T_s and the fourth term is the contribution of atmospheric upwelling radiation. In the MW region, the surface is assumed specular and therefore $|\mu_d| = \mu$.

However, in the IR region, the surface is assumed Lambertian and the surface-reflected downwelling radiation is approximated by the radiation calculated at the diffuse angle $\theta_d = 53$ degree (Liou, 1980). In both regions, the reflectivity is calculated as $r = 1 - \varepsilon$.

Integrating both sides of (14) with the channel SRF and assuming ε, r, $r_\otimes$ and B do not vary significantly within the spectral band of the sensor channel, the solution for the channel radiance, I_{ch}, is then given in a discrete form by

$$I_{ch}(\mu) = (\bar{r} I_{ch}^{\downarrow}(\mu_d) + \bar{r}_\otimes \frac{\bar{F}_\otimes}{\pi} \mathrm{T}_{ch,d}(p_0, \mu_\otimes) + \bar{\varepsilon} B(T_{s,e})) \mathrm{T}_{ch,u}(p_N, \mu) + \sum_{i=1}^{N} (\mathrm{T}_{ch,u}(p_{i-1}, \mu) - \mathrm{T}_{ch,u}(p_i, \mu)) B(T_{i,e}) , \quad (15)$$

where

$$I_{ch}^{\downarrow}(\mu_d) = \sum_{i=1}^{N} (\mathrm{T}_{ch,d}(p_i, \mu_d) - \mathrm{T}_{ch,d}(p_{i-1}, \mu_d)) B(T_{i,e}) + I_{bg} T_{ch,d}(p_0, \mu_d) .$$

In the above equation, p_i is the pressure at the i^{th} level, $\mathrm{T}_{ch,u}$ and $\mathrm{T}_{ch,d}$ are the channel upwelling and downwelling transmittance profiles as defined in (1). and $\bar{r}$, $\bar{r}_\otimes$ and $\bar{\varepsilon}$ are the averages of reflectivity and emissivity over the channel spectral band. The Planck functions are calculated at the effective skin temperature $T_{s,e}$ and air temperature $T_{i,e}$, which are defined in the equation,

$$B(T_e, \nu_0) = \int B(T, \nu) \phi(\nu) d\nu , \quad (16)$$

where ν_0 is the central frequency of the channel spectral band. The variable $I_{bg} (= B(T_{bg,e}))$ in (15) is the cosmic background radiance, equal to the Planck function at the effective cosmic background temperature $T_{bg,e}$.

For the sake of computational efficiency, the downwelling transmittances $\{ \mathrm{T}_{ch,d}(p_i, \mu_d), i = 0, N \}$ and $\mathrm{T}_{ch,d}(p_0, \mu_\otimes)$ are not calculated in the way described in Section 2.2, but are derived approximately from the upwelling transmittances $\{ \mathrm{T}_{ch,u}(p_i, \mu), 0 = 1, N \}$ in the same way as deriving the downwelling monochromatic transmittance from the upwelling monochromatic transmittance.

2.4.4 RT Solution under Cloudy Conditions

The advanced doubling and adding method (ADA) (Liu and Weng, 2006), recently developed for the cases in which the atmospheric scattering is significant, is also implemented in the RT Solution module. As in the clear-sky case, it is used to solve the channel radiance directly, assuming the optical properties of the Earth surface and clouds as well as the Planck functions do not vary significantly within the channel spectral band. The optical depth profile used in the multi-stream RT solution is derived from the channel transmittances (see Section 2.2) calculated at the satellite zenith angle. For simplicity, in the following expressions we drop off the channel subcript indicator with the understanding that the radiances and transmittances are all polychromatic channel quantities.

In the discrete ordinate form, (13) can be rewritten as

$$\begin{aligned}\mu_i \frac{dI(\tau,\mu_i)}{d\tau} &= I(\tau,\mu_i) - \varpi P(\mu_i,\mu_j) I(\tau,\mu_j) w_j - \varpi P(\mu_i,\mu_{-j}) I(\tau,\mu_{-j}) w_j - (1-\varpi) B(T) \\ -\mu_i \frac{dI(\tau,\mu_{-i})}{d\tau} &= I(\tau,\mu_{-i}) - \varpi P(\mu_{-i},\mu_j) I(\tau,\mu_j) w_j - \varpi P(\mu_{-i},\mu_{-j}) I(\tau,\mu_{-j}) w_j - (1-\varpi) B(T)\end{aligned}, \qquad (17)$$

where the solar contribution has been ignored. In (17) μ_i and w_i are Gaussian quadrature points and weights, respectively. μ_i and μ_{-i} represent the cosine of the viewing zenith angle in upward and downward directions, respectively. The repeated subscript *j* involves a summation. The phase matrix elements $P(\mu_i,\mu_j)$ and $P(\mu_i,\mu_{-j})$ are the azimuth-averaged forward and backward parts, respectively, $P(\mu_i,\mu_j) = P(\mu_{-i},\mu_{-j})$ and $P(\mu_{-i},\mu_j) = P(\mu_i,\mu_{-j})$ due to the symmetry conditions of the phase function for spherical scatterers or for randomly-oriented particles with a symmetric plane. Written in a matrix-vector form (17) becomes:

$$\frac{d}{d\tau}\begin{bmatrix}\mathbf{I_u}\\ \mathbf{I_d}\end{bmatrix} = -\begin{bmatrix}\boldsymbol{\alpha} & \boldsymbol{\beta}\\ -\boldsymbol{\beta} & -\boldsymbol{\alpha}\end{bmatrix}\begin{bmatrix}\mathbf{I_u}\\ \mathbf{I_d}\end{bmatrix} - (1-\varpi)B(T)\begin{bmatrix}\mathbf{u}^{-1}\Xi\\ -\mathbf{u}^{-1}\Xi\end{bmatrix}, \qquad (18)$$

where $\boldsymbol{\alpha}$ and $\boldsymbol{\beta}$ are *N* by *N* matrices, whose elements are

$$\alpha(\mu_i,\mu_j) = [\varpi\, P(\mu_i,\mu_j) w_j - \delta_{ij}]/\mu_i \text{ and}$$

$$\beta(\mu_i,\mu_{-j}) = \varpi\, P(\mu_i,\mu_{-j}) w_j / \mu_i, \qquad (19)$$

respectively, and δ_{ij} is the Kronecker delta. The subscripts *u* and *d* indicate upward and downward directions, respectively. **u** is a *N* by *N* matrix that has non-zero elements in its diagonal such as

$$\mathbf{u} = [\mu_1, \mu_2, ..., \mu_N]_{diagnonal}, \qquad (20)$$

Ξ is a vector of N elements as

$\Xi = [1,1,...,1]^T$.

Layer reflection, transmission and source matrices

For an infinitesimal optical depth δ_0, multiple scattering may be neglected and the reflection and transmission matrixes can be expressed, respectively, as:

$$\mathbf{r}(\delta_0) = \delta_0 \boldsymbol{\beta} \text{ and } \mathbf{t}(\delta_0) = \mathbf{E} + \boldsymbol{\alpha}\delta_0, \qquad (21)$$

where **E** is an *N* by *N* unit matrix. Using the doubling procedure, the reflection and transmission matrices for the homogeneous layer with a finite optical depth ($\delta = \delta_n = 2^n \delta_0$) can be computed by doubling the optical depth (i.e. $\delta_{i+1}/\delta_i = 2$) recursively:

$$\mathbf{r}(\delta_{i+1}) = \mathbf{t}(\delta_i)[\mathbf{E} - \mathbf{r}(\delta_i)\mathbf{r}(\delta_i)]^{-1}\mathbf{r}(\delta_i)\mathbf{t}(\delta_i) + \mathbf{r}(\delta_i),$$

and

$$\mathbf{t}(\delta_{i+1}) = \mathbf{t}(\delta_i)[\mathbf{E} - \mathbf{r}(\delta_i)\mathbf{r}(\delta_i)]^{-1}\mathbf{t}(\delta_i), \qquad (22)$$

for i = 0, n-1.

The source function matrix is computed with a new formula, which significantly improves the computation efficiency over the existing ones (Hansen, 1971). The upward layer source function can be derived as:

$$\mathbf{S_u} = [(\mathbf{E}-\mathbf{t}-\mathbf{r})B(T_1) - (B(T_2)-B(T_1))\mathbf{t} + \frac{B(T_2)-B(T_1)}{(1-\varpi g)\delta}(\mathbf{E}+\mathbf{r}-\mathbf{t})\mathbf{u}]\boldsymbol{\Xi}, \quad (23)$$

and the downward as:

$$\mathbf{S_d} = [(\mathbf{E}-\mathbf{t}-\mathbf{r})B(T_1) + (B(T_2)-B(T_1))(\mathbf{E}-\mathbf{r}) + \frac{B(T_2)-B(T_1)}{(1-\varpi g)\delta}(\mathbf{t}-\mathbf{E}-\mathbf{r})\mathbf{u}]\boldsymbol{\Xi}, \quad (24)$$

where ϖ and g are the single scattering albedo and asymmetry factor of the layer, respectively.

Upward radiance at the top of multilayer atmosphere

For an atmosphere with *n* optically homogeneous layers, the upward radiance at the top of atmosphere is calculated using the adding method, starting at the earth surface. Let $\mathbf{R_u}(k)$ denote the reflection matrix and $\mathbf{I_u}(k)$ the radiance vector at the level k in the upward direction, with k=n and k=0 representing the surface level and the top of the atmosphere, respectively. At the surface, $\mathbf{R_u}(n)$ is the surface reflection matrix and $\mathbf{I_u}(n)$ equals the surface emissivity vector multiplied by the Planck function at the effective surface temperature. The upward reflection matrix and radiance at the next level can be obtained by adding one layer from the present level:

$$\mathbf{R}(k-1) = \mathbf{r}(k) + \mathbf{t}(k)[\mathbf{E}-\mathbf{R}(k)\mathbf{r}(k)]^{-1}\mathbf{R}(k)\mathbf{t}(k), \quad (25)$$

$$\mathbf{I_u}(k-1) = \mathbf{S_u}(k) + \mathbf{t}(k)[\mathbf{E}-\mathbf{R}(k)\mathbf{r}(k)]^{-1}\mathbf{R}(k)\mathbf{S_d}(k) + \mathbf{t}(k)[\mathbf{E}-\mathbf{R}(k)\mathbf{r}(k)]^{-1}\mathbf{I_u}(k).$$

At the end of the recursive calculation, one obtains $\mathbf{R_u}(0)$ and $\mathbf{I_u}(0)$ at the top level of the atmosphere and then adds the cosmic background radiance $\mathbf{I}_{bg}$ to yield the solution

$$\mathbf{I_u} = \mathbf{I_u}(0) + \mathbf{R}_u(0)\,\mathbf{I}_{bg}. \quad (26)$$

For the viewing angle not coincident with the angles at Gaussian quadrature points, an additional stream as an extra Gaussian quadrature point associated with an integration weight of zero is inserted to have *N* quadrature points in total in either upward or downward directions. For this case, the upward intensity vector will contain the upward solutions at *N-1* quadrarture points and at the specified viewing angle.

Accuracy and efficiency

The model inter-comparisons are carried out between the doubling-adding model (Evans and Stephens 1991), VDISORT (Weng and Liu 2003), and the advanced doubling-adding method. The three solvers share the same atmospheric optic data, the same surface emissivity and reflectivity, and the same Planck function for atmosphere, surface, and the cosmic background. For 24000 simulations with various clear and cloudy cases, ADA is about 1.7 times faster than VDISORT and 61 times

faster than DA. The maximum differences of the simulated brightness temperatures between the three solvers for AMSU-A channels and 281 selected Atmospheric InfraRed Sounder (AIRS) channels are less than 0.01 Kelvin.

3 Tangent-linear, Adjoint and K-Matrix Models

For many satellite radiance applications, not only the forward model is essential, but also the capabilities to rapidly compute the radiance sensitivities with respect to the state variables. The CRTM package includes both the forward model (FW) and the tangent-linear (TL), adjoint (AD) and K-Matrix (K) models for computing the radiance sensitivities.

3.1 Tangent-linear Model

Let *F* represent the FW model for simulating the radiance vector *Y* (in intensity or brightness temperature units) for a given state vector *X*:

$$Y = F(X) . \tag{27}$$

Then the TL model may be expressed as

$$\delta Y = H(X)\delta X , \tag{28}$$

where X and δX are model inputs with δX being the perturbation of the state vector *X*. *H* is the tangent-linear operator, a matrix containing the derivatives (Jacobians) of the radiances with respect to the state variables as

$$H_{i,j} = \frac{\partial F_i}{\partial x_j} . \tag{29}$$

Thus, the i^{th} element in δY is the response of the radiance y_i to the perturbations of the state variables x_j (*j=1, n*):

$$\delta y_i = \sum_{j=1}^{n} \frac{\partial F_i}{\partial x_j}\delta x_j . \tag{30}$$

The CRTM TL model is built on the FW model source code, which can be considered as a composition of a set of functions $Z^l = F^l(Z^{l-1})$ (*l=1,K*) with $Z^0 = X$:

$$F(X) = F^K(...<F^2[F^1(Z^0 = X)]>...) , \tag{31}$$

where the superscript *l* on *Z* and *F* is an index, not an exponent. Applying the chain rule to the expression above, the TL equation (28) may be rewritten in the form,

$$\delta Y = H^K(Z^{K-1})H^{K-1}(Z^{K-2})\cdots H^l(Z^{l-1})\cdots H^1(Z^0)\delta Z^0 , \tag{32}$$

or equivalently in the form of a series of TL functions as

$$\delta Z^1 = H^1(Z^0)\delta Z^0, \delta Z^2 = H^2(Z^1)\delta Z^1, \cdots, \delta Z^l = H^l(Z^{l-1})\delta Z^{l-1}, \cdots, \delta Y = H^K(Z^{K-1})\delta Z^{K-1}, \quad (33)$$

where

$$H^l(Z^{l-1}) = \{H^l{}_{i,j}\} = \{\frac{\partial F^l{}_i}{\partial Z^{l-1}{}_j}\}$$

is the Jacobian matrix of the function F^l with respect to Z^{l-1}. The expression (33) is the basis for coding the TL model: the TL functions $\delta Z^l = H^l(Z^{l-1})\delta Z^{l-1}$ ($l=1,K$) are first constructed and coded by differentiating the corresponding FW functions $Z^l = F^l(Z^{l-1})$ ($l=1,K$) and the TL model is then the result of applying the chain operations as expressed in (33).

3.2 Adjoint Model

Let the scalar variable, J, be a function of the radiance vector $Y=F(X)$. Usually $J(Y)$ is a cost function. Its gradient with respect to the state vector X may be expressed as

$$\nabla_X J = \nabla_X Y \nabla_Y J, \quad (34)$$

where $\nabla_Y J$ is the gradient vector of the J function with respect to the radiance vector Y and $\nabla_X Y$ is a matrix whose *jth* column is the gradient of y_j with respect to X. Thus, $\nabla_X Y$ is the transpose of the Jacobian matrix H, expressed as H^T, and is the adjoint operator. Equation (34) is called the AD model (Errico, 1997).

According to the discussion in Section 4.1 and the expression (31), $J(Y)$ may also be considered as a function of the intermediate result $Z^l = F^l(F^{l-1}(...F^1(Z^0 = X)))$:

$$J(Z^l) = J(F^K(F^{K-1}(...F^{l+1}(Z^l)))).$$

Thus, by introducing an AD variable $\delta^* Z^l$, defined as the gradient of the J function with respect to Z^l (Giering and Kaminski, 1998),

$$\delta^* Z^l = \nabla_{Z^l} J(Z^l), \quad (35)$$

and noticing that $\delta^* Y = \nabla_Y J$ and $\delta^* X = \nabla_X J$ according to the definition of the AD variable, we can rewrite the AD model (34) into the form,

$$\begin{aligned} \delta^* X &= H(X)^T \delta^* Y \\ &= (H^1)^T (H^2)^T \cdots (H^K)^T \delta^* Y \end{aligned}, \quad (36)$$

where X and $\delta^* Y$ are the AD model inputs. Equivalently we can also write (36) in the form of a series of AD functions as

$$\delta^* Z^{K-1} = (H^K)^T \delta^* Y, \delta^* Z^{K-2} = (H^{K-1})^T \delta^* Z^{K-1}, \cdots, Z^1 = (H^2)^T \delta^* Z^2, \delta^* X = (H^1)^T \delta^* Z^1. \quad (37)$$

This expression is the basis for coding the AD model: the AD functions $\delta^* Z^{l-1} = (H^l)^T \delta^* Z^l$ ($k=1,K$) are first constructed and coded by manipulating the corresponding TL functions $\delta Z^l = H^l(Z^{l-1})\delta Z^{l-1}$ ($l=1,K$) (Giering and Kaminski, 1998) and the AD model is then the result of applying the chain operations according to (37). Note that compared with the TL model, the adjoint model is operated in the reverse order, with $(H^K)^T \delta^* Y$ evaluated first, yielding the intermediate result $\delta^* Z^{K-1}$ as the input for the next operation $(H^{K-1})^T \delta^* Z^{K-1}$, and so on. In the end, the net result is in the AD vector $\delta^* X$, whose *jth* element $\delta^* x_j$ is given by

$$\delta^* x_j = \sum_{i=1}^{m} \frac{\partial F_i}{\partial x_j} \delta^* y_i , \tag{38}$$

where the summation is over all the radiance channels.

3.3 K-Matrix Model

From Section 4.2, we can see that the AD model does not directly output the Jacobian matrix *H* unless extra steps are taken to separate the terms in (38). It is the K-Matrix model that provides the Jacobian matrix. The K-Matrix model is derived from the AD model by adding an additional step in the AD model to save each of the terms in (38) in a separate storage unit in the so-called K matrix. In the end of the model computation, the K matrix contains the following content:

$$X\_K = [h_1 \delta^* y_1, h_2 \delta^* y_2, ..., h_m \delta^* y_m] \tag{39}$$

where $\delta^* y_i$ ($i = 1, m$), together with the state vector *X*, are the K-Matrix model inputs and h_i is the transpose of the i^{th} row of the *H* matrix:

$$h_i = [\frac{\partial F_i}{\partial x_1}, \frac{\partial F_i}{\partial x_2}, ..., \frac{\partial F_i}{\partial x_n}]^T . \tag{40}$$

Thus, if we set the input variables $\delta^* y_i = 1$ ($i=1,m$) when running the K-Matrix model, the returned matrix *X_K* contains the Jacobians.

3.4 Naming Convention

It can be seen in the previous two Sections, the TL and AD variables and functions are paired with the FW variables and functions. For instance, the TL and AD variables δX and $\delta^* X$ are paired with the FW variable *X*. However, in the Fortran language, the symbols δ and δ^* are not allowed for variable and function routine names. Thus, the following naming convention is in order for naming the TL and AD variables and routine names. The TL and AD variables and function routines are named by adding the suffixes "_TL" and "_AD" to those of their FW model counterparts. For example, if *var* and *routine* represent the FW variable and routine names respectively, the corresponding TL and AD variables and routines are named as *var_TL*, *routine_TL*, *var_AD*, and *routine_AD*, respectively.

4 User Interfaces

The user interface comprises primarily a set of interfaces of the user callable routines. These routines are listed in Table 4. The key interface arguments for inputs and outputs are listed in Table 5. Note that the listed arguments are all of the derived types (structures), whose definitions are given in Appendix. The required coefficient files, whose filenames need to be specified by the user during the CRTM initialization, are listed in Table 6.

The interface routines can be put into three categories: the CRTM initialization and destroy routines, the model routines for the FW, TL, AD and K_Matrix model computations and the utility routines such as the sensor/channel selection routine and memory allocation/deallocation routines for the structure variables that contain pointer arrays. In the following we provide brief descriptions for some of the user interface routines.

Initialization routine `CRTM_Init`

Calling example:

```
Error_Status = CRTM_Init( &
    ChannelInfo,                          & ! output
    SpcCoeff_File     = SpcCoeff_File,    & ! optional input
    TauCoeff_File     = TauCoeff_File,    & ! optional input
    AerosolCoeff_File = AerosolCoeff_File,& ! optional input
    CloudCoeff_File   = ScatterCoeff_File,& ! optional input
    EmisCoeff_File    = EmisCoeff_File)     ! optional input
```

Description:

Before calling the CRTM model routines, the user must call the initialization routine *CRTM_Init*, which loads the coefficient files and sets the initial content of the structure *ChannelInfo*. The names of the coefficient files may be specified by the operational string arguments. If the optional string names are not present, the default names are used: *SpcCoeff .bin*, *TauCoeff.bin AerosolCoeff .bin*, and *ScatterCoeff.bin*. In this example the content of *ChannelInfo* will be set to include all the channels and sensors defined in the coefficient data files *SpcCoeff* and *TauCoeff*. Note that after the initialization, the user may use the channel selection routine *CRTM_Set_ChannelInfo* to change the content of the structure *ChannelInfo* for a different set of sensors and channels.

Sensor/channel selection routine CRTM_Set_ChannelInfo

Calling example:

```
Error_Status = CRTM_Set_ChannelInfo( Sensor_Descriptor, & ! input
                                     ChannelInfo)   ! ouput
```

or

```
Error_Status = CRTM_Set_ChannelInfo( Sensor_Descriptors, & ! input
                                     Sensor_Channels, & ! input
                                     ChannelInfo)       ! output
```

Description:

This routine is used to set the content of the structure ChannelInfo for a selection of the channels and sensors in the subsequent model calculations. In the first calling example, ChannelInfo is set to include all the channels of the sensor specified by the string variable Sensor_Descriptor. For instance, if Sensor_Descriptor contains "amsua_n16", the returned ChannelInfo holds the spectral information only for the channels of the AMSUA sensor on the NOAA-16 satellite. In the second calling example, ChannelInfo is set for the selected channels and sensors described by both the index array Sensor_Channels and the string array Sensor_Descriptors. The *ith* element of the index array Sensor_Channels contains a channel number of the sensor whose identification is described by the string name stored in the *ith* element of the array Sensor_Descriptors. The second calling example allows the user to select a subset of the channels and sensors defined in the coefficient data files *SpecCoeff* and *TauCoeff*.

Forward model routine CRTM_Forward

Calling example:

```
Error_Status = CRTM_Forward( Atmosphere,   &  ! input
                             Surface,      &  ! input
                             GeometryInfo, &  ! input
                             ChannelInfo,  &  ! input
                             RTSolution,   &  ! output
                             Options = Options) ! optional input
```

Descriptions:

The forward model is called to simulate satellite radiances for a given atmospheric and surface state, described by both of the structure variables Atmosphere and Surface. The *geometryInfo* structure variable contains the satellite and solar zenith angles. The structure variable *Channelinfo* specifies the sensors and channels. The optional input variable Options contains the user-supplied surface emissivity/reflectivity spectrum for the intended channels. If the Options variable is not present, the spectrum is computed internally. The model outputs (radiances and brightness temperatures) are stored in the structure *RTSolution*. If the structure member *Layer_Optical_Depth* in *RTSolution* has been allocated, *RTSolution* also contains the layer optical depths.

Jacobian model routine K-Matrix

Calling example:

```
  Error_Status = CRTM_K_Matrix( Atmosphere, & ! input
                                Surface, & ! input
                               RTSolution_K, & ! input
                               GeometryInfo, & ! input
                                ChannelInfo, & ! input
                               Atmosphere_K, & ! input/output
                                  Surface_K, & ! input/output
                                RTSolution , & ! output
                              Options = Options ) ! optional output
```

Description:

The K_Matrix model is called to compute radiance derivatives with respective to the state variables (Jacobians) as well as the radiances. The structure variables *Atmosphere*, *Surface*, *GeometryInfo*, *ChannelInfo*, *RTsolution* and *Options* are used in the same way as those in the forward model call. The K-Matrix variables *Atmosphere_K* and *Surface_K* are arrays with a channel dimension, holding the returned Jaconbians. For example, the variable *Atmosphere_K*(i)*%Temperature*(k) contains the radiance or brightness temperature Jacobian for the *ith* channel with respect to the air temperature at the *kth* layer. The structure variable *RTSolution_K* is an input variable, which determines the Jacobian units. If the user sets *RTSolution_K%Radiance* = 1 and *RTSolution_K%Brightness_temperature* = 0, the model outputs are radiance Jacobians; if *RTSolution_K%Radiance* = 0 and *RTSolution_K%Brightness_temperature* = 1, the outputs are brightness temperature Jacobians.

CRTM destruction routine CRTM_Destroy

Calling example:

```
Error_Status = CRTM_Destroy( ChannelInfo )
```

Description:

The destruction routine *CRTM_Destroy* is called to deallocate memory occupied by the CRTM data variables. After this call, it is no longer valid to call CRTM model routines unless the CRTM is reinitialized with the routine *CRTM_Init*.

Subprogram Name	Description
CRTM_Init	Initialize CRTM and load CRTM coefficient data.
CRTM_Set_ChannelInfo	Select sensors and channels
CRTM_Forward	CRTM forward model
CRTM_Tangent_Linear	CRTM tangent-linear model
CRTM_Adjoint	CRTM Adjoint model
CRTM_K_Matrix	CRTM K_Matrix (Jacobian) model
CRTM_Destroy	Release memory used by CRTM
Memory allocation/deallocate subprograms	
CRTM_Allocate_Atmosphere CRTM_Destroy_Atmosphere	Allocate and deallocate memory for the Atmosphere structure pointer array members.
CRTM_Allocate_Surface CRTM_Destroy_Surface	Allocate and deallocate memory for the Surface structure pointer array members.
CRTM_Allocate_RTSolution CRTM_Destroy_RTSolution	Allocate and deallocate memory for the RTSolution structure pointer array members.
CRTM_Allocate_Options CRTM_Destroy_Options	Allocate and deallocate memory for the Options structure pointer array members.

Table 4 CRTM interface routines

Type name	Description
Atmosphere	The forward (tangent-linear, adjoint or K-Matrix) variable of the atmospheric state
Cloud	The forward (tangent-linear, adjoint or K-Matrix) variable of the cloud profiles
Surface	The forward (tangent-linear, adjoint or K-Matrix) variable of the surface data
RTSolution	The forward (tangent-linear, adjoint or K-Matrix) variable holding the RT solutions.
ChannelInfo	Contains selected sensor/channel information for subsequent calls to the CRTM models.
GeometryInfo	Contains satellite geometry data such as sensor and solar zenith angles.
Options	Contains optional variables such as the user-provided surface emissivity.

Table 5 Structure variable types used for the interface arguments (see Appendix for their definitions)

Coefficient data file	Description
Spectral coefficient (SpcCoeff) file	Contains sensor spectral information (Sensor dependent)
Optical depth (TauCoeff) coefficient file	Contains transmittance coefficient data (sensor dependent)
Cloud coefficient (CloudCoeff) file	Cloud optical parameters and lookup tables such as mass extinction coefficients, single scattering albedo, asymmetry factors and Legendre expansion coefficients.
Surface Emissivity coefficient (EmisCoeff) file	Contains coefficient data for computing infrared ocean surface emissivity
Aerosol coefficient (AerosolCoeff) file	Currently a dummy file (placeholder for aerosol component)

Table 6 CRTM coefficient data files

.

References

Carter, C., Q. Liu, W. Yang, D. Hommel, and W. Emery, 2002: Net heat flux, visible/infrared imager/radiometer suite algorithm theoretical basis document. Available on http://npoesslib.ipo.noaa.gov/u_listcategory_v3.php?35.

Cox, C. and W. Munk, 1954, Statistics of the sea surface derived from sun glitter. *J. Mar. Res*. **13** 198-227.

Clough, S. A., M. J. Iacono and J. L. Moncet, 1992: Line-by-line calculations of atmospheric fluxes and cooling rates: application to water vapor. *J. Geophys. Res*. **97**, 15761-15785.

English, S.J. and T.J. Hewison, 1998: A fast generic millimetre wave emissivity model. *Microwave Remote Sensing of the Atmosphere and Environment Proc. SPIE* **3503** *22-30.*

Errico, R. M., 1997: What is an adjoint model. *Bull. Amer. Meteo. Soci*., **78**, 2577-2591.

Evans, K. F. and G. L. Stephens, 1991: A new polarized atmospheric radiative transfer model. *J. Quant. Spectrosc. Radiat. Transfer*, **46**, 413-423.

Giering, R. and T. Kaminski, 1998: Recipes for Adjoint Code Construction. *ACM Transation on Mathematical Software*, **24,** 437-474.

Hansen, J.E., 1971: Multiple scattering of polarized light in planetary atmosphere. *J. Atmos. Sci*., **28**, 120-125.

Kleespies, T. J., P. V. Delst, L. M. McMillin, J. Derber, 2004: Atmospheric Transmittance of an Absorbing Gas. 6. OPTRAN Status Report and Introduction to the NESDIS/NCEP Community Radiative Transfer Model, *Appl. Opt*., **43**, 3103-3109.

Liou, K, 1980: An introduction to atmospheric radiation, Academic. Press, Inc, New York.

Liu, Q and F. Weng, 2006: Advanced Doubling-Adding Method for Radiative Transfer in Planetary Atmospheres. *J. Atmos. Sci*, accepted.

McMillin, L. M., L. J. Crone, M. D. Goldberg, and T. J. Kleespies, 1995: Atmospheric transmittance of an absorbing gas. 4. OPTRAN: a computationally fast and accurate transmittance model for absorbing gases with fixed and variable mixing ratios at variable viewing angles. *Appl. Opt*. **34**, 6269 - 6274.

Saunders, R. M., M. Matricardi, and P. Brunel, 1999: An improved fast radiative transfer model for assimilation of satellite radiance observation, *QJRMS*, **125**, 1407-1425.

Weng, F., B. Yan, and N. Grody, 2001: A microwave land emissivity model, *Geophys. Res.,* **106**, 20,115-20,123.

Weng, F., and Q. Liu, 2003: Satellite Data Assimilation in Numerical Weather Prediction Models, Part I: Forward Radiative Transfer and Jocobian Modeling in Cloudy Atmospheres. *J. Atmos. Sci.,* **60**, 2633 – 2646.

Weng, F., Y. Han, P. van Delst, Q. Liu, and B. Yan, 2005: JCSDA Community radiative transfer model (CRTM), *Technical Proceedings of Fourteenth International ATOVS Study Conference*, Beijing

Wu , X. and W. L. Smith, 1997: Emissivity of rough sea surface for 8-13 μm: modeling and verification. *Appl. Opt*., **36**, 2609-2619.

Xiong, X. and L.M. McMillin, 2005: An Alternative to the Effective Transmittance Approach for Calculating Polychromatic Transmittances in Rapid Transmittance Models, *Appl. Opt*., **44**, 67-76 (2005).

Yan, B., F. Weng, K. Okamoto, 2004: Improved Estimation of Snow Emissivity from 5 to 200 GHz. *8th Specialist Meeting on Microwave Radiometry and Remote Sensing Applications*,24-27 February, 2004, Rome, Italy.

Yang, P., B.-C. Gao, B. A. Baum, W. Wiscombe, Y. Hu, S. L. Nasiri, A. Heymsfield, G. McFarquhar, and L. Miloshevich, 2001: Sensitivity of cirrus bidirectional reflectance in MODIS bands to vertical inhomogeneity of ice crystal habits and size distributions. *J. Geophys. Res*., **106**, 17267-17291.

Appendix A Definitions of CRTM Derived Types (Structures)

Listed in the following Tables are definitions of the structure variables used in the user interface. The letters J, L, K, Nc, Na in the tables represent the numbers of absorbing gases, channels, layers, cloud types and aerosol types, respectively. The parameter *fp_kind* is a generic kind type for declaring floating-point variables.

A.1 Atmosphere structure.

Member	Type	Dimension	Initial value	Description
Max_Layers	Integer	Scalar	0	Maximum number of atmospheric layers
N_Layers	Integer	Scalar	0	Number of atmospheric layers.
N_Absorbers	Integer	Scalar	0	Number of atmospheric absorbers (H2O, O3, etc.)
Max_Clouds	Integer	Scalar	0	Maximum number of clouds
N_Clouds	Integer	Scalar	0	Number of clouds
Max_Aerosols	Integer	Scalar	0	Maximum number of aerosol types
N_Aerosols	Integer	Scalar	0	Number of aerosol types
Absorber_ID	Integer pointer	Rank-1 (J)	NULL()	A flag value to identify a molecular species in the absorber profile
Pressure	Real(fp_kind) Pointer	Rank-1 (L)	NULL()	Layer pressure profile (hPa)
Level_Pressure	Real(fp_kind) Pointer	Rank-1 (0:L)	NULL()	Pressure boundaries of the layer pressure profile (hPa)
Temperature	Real(fp_kind) Pointer	Rank-1 (L)	NULL()	Layer temperature profile (K)
Absorber	Real(fp_kind) Pointer	Rank-2 (L x J)	NULL()	Layer absorber amount profiles
Cloud	CRTM_Cloud_type Pointer	Rank-1 (Nc)	NULL()	Structure containing cloud data
Aerosol	CRTM_Aerosol_type Pointer	Rank-1 (Na)	NULL()	Structure containing aerosol data, **currently not used**.

A.2 Cloud structure

Member name	Type	Dimension	Initial value	Description
N_Layers	Integer	Scalar	0	Maximum number of atmospheric layers
Type	Integer	Scalar	NO_CLOUD	Flag value indicating the cloud type
Effective_Radius	Real(fp_kind) Pointer	Rank-1 (L)	NULL()	The effective radius of the cloud particle size distribution
Water_Content	Real(fp_kind) Pointer	Rank-1 (L)	NULL()	The water content of the cloud

A.3 Surface structure

Member Name	Type	Dimension	Initial or default value	Description
Gross type of surface determined by coverage				
Land_Coverage	Real(fp_kind)	Scalar	ZERO	Fraction of surface that is of the land surface type
Water_Coverage	Real(fp_kind)	Scalar	ZERO	Fraction of surface that is of the water surface type
Snow_Coverage	Real(fp_kind)	Scalar	ZERO	Fraction of surface that is of the snow surface type
Ice_Coverage	Real(fp_kind)	Scalar	ZERO	Fraction of surface that is of the ice surface type
Land surface type data				
Land_Type	Integer	Scalar	GRASS_SOIL	The land surface type. See A3 for the valid types
Land_Temperature	Real(fp_kind)	Scalar	283.0	The land surface temperature (K).
Soil_Moisture_Content	Real(fp_kind)	Scalar	0.05	The volumetric water content of the soil (g.cm^-3).
Canopy_Water_Content	Real(fp_kind)	Scalar	0.05	The gravimetric water content of the canopy (g.cm^-3).
Vegetation_Fraction	Real(fp_kind)	Scalar	0.3	The vegetation fraction of the surface.
Soil_Temperature	Real(fp_kind)	Scalar	283.0	The soil temperature (K).
Water type data				
Water_Type	Integer	Scalar	SEA_WATER	The water surface type.
Water_Temperature	Real(fp_kind)	Scalar	283.0	The water surface temperature (K).
Wind_Speed	Real(fp_kind)	Scalar	5.0	Surface wind speed (m.s^-1)
Wind_Direction	Real(fp_kind)	Scalar	0.0	Surface wind direction in degree east from North
Salinity	Real(fp_kind)	Scalar	33.0	Water salinity (ppmv)
Snow surface type data				
Snow_Type	Integer	Scalar	NEW_SNOW	The snow surface type. See A3 for the valid types
Snow_Temperature	Real(fp_kind)	Scalar	263.0	The snow surface temperature (K).
Snow_Depth	Real(fp_kind)	Scalar	50.0	The snow depth (mm).
Snow_Density	Real(fp_kind)	Scalar	0.2	The snow density (g.cm^-3)
Snow_Grain_Size	Real(fp_kind)	Scalar	2.0	The snow grain size (mm).
Ice surface type data				
Ice_Type	Integer		FRESH_ICE	The ice surface type.
Ice_Temperature	Real(fp_kind)	Scalar	263.0	The ice surface temperature (K).
Ice_Thickness	Real(fp_kind)	Scalar	10.0	The thickness of the ice (mm)
Ice_Density	Real(fp_kind)	Scalar	0.9	The ice density (g.cm^-3)
Ice_Roughness	Real(fp_kind)	Scalar	ZERO	Measure of the surface roughness of the ice
SensorData containing channel brightness temperatures				
SensorData	CRTM_SensorData_Type	Scalar	See Table A4	Satellite sensor data required for some surface algorithms. Can be left empty.

A.4 SensorData structure

Member name	Type	Dimension	Initial value	Description
n_Channels	Ingeter	Scalar	0	Number of the channels
Sensor_ID	Integer	Scalar	INVALID	WMO sensor ID (see A3.5 for the valid sensor ID)
Tb	Real(fp_kind) pointer	Rank-1 (L)	NULL()	The sensor brightness temperatures (K).

A.5 GeometryInfo structure

Member name	Type	Dimension	Initial value	Description
Sensor_Zenith_Angle	Real(fp_kind)	Scalar	ZERO	The sensor zenith angle (degrees)
Satellite_Height	Real(fp_kind)	Scalar	800km (Default)	Height of the satellite above the Earth surface (for AMSUA/B sensors only)
Source_Zenith_Angle	Real(fp_kind)	Scalar	FP_INVALID	Solar zenith angle (for IR sensors)

A.6 ChannelInfo structure

Member name	Type	Dimension	Initial value	Description
n_Channels	Integer	Scalar	0	Total number of channels.
Channel_Index	Integer pointer	Rank-1 (L)	NULL()	The index of the channels loaded during CRTM initialization.
Sensor_Channel	Integer pointer	Rank-1 (L)	NULL()	The sensor channel number
Sensor_Descriptor	Character pointer	Rank-1 (L)	NULL()	A character string containing a description of the satellite and sensor name
NCEP_Sensor_ID	Integer pointer	Rank-1 (L)	NULL()	The NCEP/EMC "in-house" value used to distinguish between different sensor/platform combinations.
WMO_Satellite_ID	Integer pointer	Rank-1 (L)	NULL()	The WMO Satellite ID number
WMO_Sensor_ID	Integer pointer	Rank-1 (L)	NULL()	The WMO Sensor ID number

A.7 RTSolution structure

Member name	Type	Dimension	Initial value	Description
Radiance	REAL(fp_lind)	Scalar	ZERO	Channel radiance (mW/(m2.sr.cm-1))
Brightness Temperatuer	REAL(fp_lind)	Scalar	ZERO	Brightness temperature (K)
Surface_Emissivity	REAL(fp_lind)	Scalar	ZERO	Surface emissivity at the observation zenith angle
n_Layers	Integer	Scalar	0	Number of layers
Layer_Optical_Depth	Real(fp_kind) pointer	Rank-1 (K)	NULL()	Optional. If this array is allocated, it contains layer total optical depth profile, if not allocated, access this array is an invalid operation.

NESDIS 98 NOAA-L and NOAA-M AMSU-A Antenna Pattern Corrections. Tsan Mo, August 2000.

NESDIS 99 The Use of Water Vapor for Detecting Environments that Lead to Convectively Produced Heavy Precipitation and Flash Floods. Rod Scofield, Gilberto Vicente, and Mike Hodges, September 2000.

NESDIS 100 The Resolving Power of a Single Exact-Repeat Altimetric Satellite or a Coordinated Constellation of Satellites: The Definitive Answer and Data Compression. Chang-Kou Tai, April 2001.

NESDIS 101 Evolution of the Weather Satellite Program in the U.S. Department of Commerce - A Brief Outline. P. Krishna Rao, July 2001.

NESDIS 102 NOAA Operational Sounding Products From Advanced-TOVS Polar Orbiting Environmental Satellites. Anthony L. Reale, August 2001.

NESDIS 103 GOES-11 Imager and Sounder Radiance and Product Validations for the GOES-11 Science Test. Jaime M. Daniels and Timothy J. Schmit, August 2001.

NESDIS 104 Summary of the NOAA/NESDIS Workshop on Development of a Coordinated Coral Reef Research and Monitoring Program. Jill E. Meyer and H. Lee Dantzler, August 2001.

NESDIS 105 Validation of SSM/I and AMSU Derived Tropical Rainfall Potential (TRaP) During the 2001 Atlantic Hurricane Season. Ralph Ferraro, Paul Pellegrino, Sheldon Kusselson, Michael Turk, and Stan Kidder, August 2002.

NESDIS 106 Calibration of the Advanced Microwave Sounding Unit-A Radiometers for NOAA-N and NOAA-N=. Tsan Mo, September 2002.

NESDIS 107 NOAA Operational Sounding Products for Advanced-TOVS: 2002. Anthony L. Reale, Micheal W. Chalfant, Americo S. Allergrino, Franklin H. Tilley, Michael P. Ferguson, and Michael E. Pettey, December 2002.

NESDIS 108 Analytic Formulas for the Aliasing of Sea Level Sampled by a Single Exact-Repeat Altimetric Satellite or a Coordinated Constellation of Satellites. Chang-Kou Tai, November 2002.

NESDIS 109 Description of the System to Nowcast Salinity, Temperature and Sea nettle (*Chrysaora quinquecirrha*) Presence in Chesapeake Bay Using the Curvilinear Hydrodynamics in 3-Dimensions (CH3D) Model. Zhen Li, Thomas F. Gross, and Christopher W. Brown, December 2002.

NESDIS 110 An Algorithm for Correction of Navigation Errors in AMSU-A Data. Seiichiro Kigawa and Michael P. Weinreb, December 2002.

NESDIS 111 An Algorithm for Correction of Lunar Contamination in AMSU-A Data. Seiichiro Kigawa and Tsan Mo, December 2002.

NESDIS 112 Sampling Errors of the Global Mean Sea Level Derived from Topex/Poseidon Altimetry. Chang-Kou Tai and Carl Wagner, December 2002.

NESDIS 113 Proceedings of the International GODAR Review Meeting: Abstracts. Sponsors: Intergovernmental Oceanographic Commission, U.S. National Oceanic and Atmospheric Administration, and the European Community, May 2003.

NESDIS 114 Satellite Rainfall Estimation Over South America: Evaluation of Two Major Events. Daniel A. Vila, Roderick A. Scofield, Robert J. Kuligowski, and J. Clay Davenport, May 2003.

NESDIS 115 Imager and Sounder Radiance and Product Validations for the GOES-12 Science Test. Donald W. Hillger, Timothy J. Schmit, and Jamie M. Daniels, September 2003.

NESDIS 116 Microwave Humidity Sounder Calibration Algorithm. Tsan Mo and Kenneth Jarva, October 2004.

NOAA SCIENTIFIC AND TECHNICAL PUBLICATIONS

The National Oceanic and Atmospheric Administration **was established as part of the Department of Commerce on October 3, 1970. The mission responsibilities of NOAA are to assess the socioeconomic impact of natural and technological changes in the environment and to monitor and predict the state of the solid Earth, the oceans and their living resources, the atmosphere, and the space environment of the Earth.**

The major components of NOAA regularly produce various types of scientific and technical information in the following types of publications

PROFESSIONAL PAPERS - Important definitive research results, major techniques, and special investigations.

CONTRACT AND GRANT REPORTS - Reports prepared by contractors or grantees under NOAA sponsorship.

ATLAS - Presentation of analyzed data generally in the form of maps showing distribution of rainfall, chemical and physical conditions of oceans and atmosphere, distribution of fishes and marine mammals, ionospheric conditions, etc.

TECHNICAL SERVICE PUBLICATIONS - Reports containing data, observations, instructions, etc. A partial listing includes data serials; prediction and outlook periodicals; technical manuals, training papers, planning reports, and information serials; and miscellaneous technical publications.

TECHNICAL REPORTS - Journal quality with extensive details, mathematical developments, or data listings.

TECHNICAL MEMORANDUMS - Reports of preliminary, partial, or negative research or technology results, interim instructions, and the like.